



**HAL**  
open science

## Seasonal and diurnal ozone variations

Nicola Schneider, Franck Selsis, Joachim Urban, Olivier Lezeaux, Jérôme de La Noë, P. Ricaud

► **To cite this version:**

Nicola Schneider, Franck Selsis, Joachim Urban, Olivier Lezeaux, Jérôme de La Noë, et al.. Seasonal and diurnal ozone variations. *Journal of Atmospheric Chemistry*, 2005, 50 (1), pp.25-47. 10.1007/s10874-005-1172-z . hal-00256287

**HAL Id: hal-00256287**

**<https://hal.science/hal-00256287>**

Submitted on 13 Sep 2021

**HAL** is a multi-disciplinary open access archive for the deposit and dissemination of scientific research documents, whether they are published or not. The documents may come from teaching and research institutions in France or abroad, or from public or private research centers.

L'archive ouverte pluridisciplinaire **HAL**, est destinée au dépôt et à la diffusion de documents scientifiques de niveau recherche, publiés ou non, émanant des établissements d'enseignement et de recherche français ou étrangers, des laboratoires publics ou privés.



Distributed under a Creative Commons Attribution 4.0 International License

# Seasonal and Diurnal Ozone Variations: Observations and Modeling

NICOLA SCHNEIDER<sup>1</sup>, FRANCK SELSIS<sup>2</sup>, JOACHIM URBAN<sup>1</sup>, OLIVIER LEZEAUX<sup>3</sup>, JÉRÔME DE LA NOË<sup>1</sup> and PHILIPPE RICAUD<sup>1</sup>

<sup>1</sup>OASU, Bordeaux, France, e-mail: schneider@obs.u-bordeaux1.fr

<sup>2</sup>INTA-CSIC, Madrid, Spain

<sup>3</sup>Noveltis, Toulouse, France

**Abstract.** Ozone mixing ratios observed by the Bordeaux microwave radiometer between 1995 and 2002 in an altitude range 25–75 km show diurnal variations in the mesosphere and seasonal variations in terms of annual and semi-annual oscillations (SAO) in the stratosphere and in the mesosphere. The observations with 10–15 km altitude resolution are presented and compared to photochemical and transport model results.

Diurnal ozone variations are analyzed by averaging the years 1995–1997 for four representative months and six altitude levels. The photochemical models show a good agreement with the observations for altitudes higher than 50 km. Seasonal ozone variations mainly appear as an annual cycle in the middle and upper stratosphere and a semi-annual cycle in the mesosphere with amplitude and phase depending on altitude. Higher resolution (2 km) HALOE (halogen occultation experiment) ozone observations show a phase reversal of the SAO between 44 and 64 km. In HALOE data, a tendency for an opposite water vapour cycle can be identified in the altitude range 40–60 km.

Generally, the relative variations at all altitudes are well explained by the transport model (up to 54 km) and the photochemical models. Only a newly developed photochemical model (1-D) with improved time-dependent treatment of water vapour profiles and solar flux manages to reproduce fairly well the absolute values.

**Key words:** diurnal ozone variations, mesospheric ozone, modelling, seasonal ozone variations, stratospheric ozone

## 1. Introduction

The investigation of seasonal ozone cycles in the stratosphere and mesosphere as well as diurnal ozone variations in the mesosphere has often been seen as a useful probe for photochemical and/or transport models (Pallister and Truck, 1983) and a number of observed variations have already been analyzed (see e.g., Ricaud *et al.* (1991) and references therein). So far, the majority of studies – in particular those investigating diurnal ozone variations – focused on short time intervals (timescales of days or months) in order to be able to resolve small ozone fluctuations or because only a limited data set was available (Clancy *et al.*, 1987; Bjarnason *et al.*, 1987; Huang *et al.*, 1997). The general outcome is that relative diurnal ozone variations in the mesosphere are well reproduced (within 5% over 24<sup>h</sup> according to Connor

*et al.*, 1994) but all models predict less ozone than actually observed (Froidevaux *et al.*, 1985; Eluszkiewicz and Allen, 1993).

Seasonal ozone variations at mid- and high-latitudes were found in the form of multiannual cycles in the stratosphere and mesosphere. While lower stratospheric variations have their origin in various phenomena (for example chemical ozone destruction in the polar vortex linked to stratospheric dynamics), middle stratosphere variabilities are mainly due to transport phenomena. At higher altitudes – namely the upper stratosphere and mesosphere – seasonal ozone oscillations are not well studied. In particular, a semi-annual cycle which has been observed in the mesosphere can be caused by various mechanisms such as temperature and solar flux variability (Allen *et al.*, 1984; Nagahama *et al.*, 2003) or possibly horizontal transport (Bevilacqua *et al.*, 1990).

In this paper, we make use of the long-term monitoring database of the Bordeaux microwave radiometer (1995–2003) to perform a statistical approach in order to investigate diurnal and seasonal ozone variations in the time period from January 1995 to December 1997. The data acquisition process is shortly presented in Section 2. Two photochemical models and one chemical transport atmospheric model reproducing the observed variabilities at different altitudes are described in Section 3. A comparison of diurnal ozone changes with model results is given in Section 4, a study of seasonal ozone variations is presented in Section 5. In the latter two sections, we focus on a recently developed photochemical model (Selsis, 2000) which is used as a general tool to describe planetary atmospheres. Section 6 summarizes the paper.

## 2. Data

Since January 1995, an ozone line at 110.836 GHz is observed with a ground-based microwave radiometer at the Floirac site of the Observatoire Aquitain des Sciences de l'Univers (OASU), Bordeaux/France (44.83°N, 0.52°W), belonging to the primary Alpine stations of the Network for the Detection of Stratospheric Change (NDSC). Ozone profiles are retrieved from the emission spectra using the optimal estimation method (Rodgers, 1976) and are calculated within atmospheric layers of 5-km width in which the volume mixing ratio is assumed to be constant. The retrieval grid consists of 20 layers between 0 and 100 km. The vertical resolution changes from 10 km in the middle stratosphere up to 15 km in the upper mesosphere for a 2-h integrated spectrum. The exploitable altitude range is determined to be 25–75 km (Schneider *et al.*, 2003). The a priori contribution is <5% at 25 km and 15% at 75 km.

The instrument, observing technique, and error budget are described in detail in de La Noë *et al.* (1998), instrumental improvements, the retrieval process and a validation analysis using other ground-based instruments (microwave radiometer in Bern, lidar at the Haute-Provence Observatory) as well as satellites (HALOE<sup>1</sup>, MLS<sup>2</sup>, SAGE-II<sup>3</sup>) are found in Schneider *et al.* (2003).

The data presented in this paper were obtained between January 1995 and December 1997 with the Bordeaux ozone microwave radiometer. Observations were performed continuously, weather and hardware permitting. Due to the measurement process, the minimum time resolution of an ozone profile is 2 h.

The error budget of such a profile is given in Figure 4 in Schneider *et al.* (2003): The systematic error reaches its maximum (0.5 ppmv) around 40 km and is well below 0.2 ppmv in the mesosphere (which corresponds to a relative error smaller than 8% in the whole altitude range 25–75 km.) The average total error is of the order of 0.6–0.8 ppmv in the stratosphere and around 0.5 ppmv for the mesosphere. Here, the relative error with respect to a standard model profile strongly increases with altitude and goes up to 85% at 75 km.

### 3. The Models

#### 3.1. INTRODUCTION

In this section, we introduce the models used in the following sections. The zero-dimensional (0-D) model (Ricaud *et al.*, 1994; Ricaud *et al.*, 1996) is a photochemical model which does not take into account transport phenomena. The one-dimensional (1-D) model (Selsis, 2000) is a new time-dependent photochemical model, developed particularly for simulating the chemical evolution of the Earth's atmosphere. The three-dimensional (3-D) model (Chipperfield *et al.*, 1996) is a chemical transport model. Here, it is only used for the analysis of seasonal ozone variations.

#### 3.2. THE 0-D OR BOX MODEL

This model<sup>4</sup> is constrained by a climatological atmosphere constant over the whole year, except for temperature and pressure which are taken from the CIRA86 profiles (Barnett and Corney, 1985; Rees *et al.*, 1990) according to the respective month and the Bordeaux latitude. The different altitude/pressure levels are radiatively coupled by the calculated rate of photodissociation. The solar flux intensity is taken from Brasseur and Simon (1981). The model considers 20 chemical species from the odd  $O_x$ ,  $HO_x$ ,  $NO_x$ , and  $ClO_x$  families.

The concentrations of the long-lived species which do not show a significant diurnal variation ( $CH_4$ ,  $H_2$ ,  $N_2O$ , CFCs) are initialized by a standard climatology. The  $H_2O$  profile is fixed to 4.5 ppmv in the whole middle atmosphere, i.e. very dry stratosphere. The model has a vertical resolution of 2 km and covers the altitude range 0–75 km.

#### 3.3. THE 1-D MODEL

This model is one-dimensional with the altitude used as parameterization. It contains the gas phase chemistry for 35 chemical species, including oxygen, hydrogen,

nitrogen, and chlorine families. The chemical reaction velocities originate from the JPL 2000 catalog (Sander *et al.*, 2000).

The vertical transport of species includes molecular and turbulent diffusion. The solar spectrum used for the calculation of photodissociation rates is taken from SUSIM<sup>5</sup> onboard UARS<sup>6</sup> for the 110–400 nm range (Floyd *et al.*, 1998; Huebner *et al.*, 1992). Such daily measurements take into account variations of the solar irradiation during the period of O<sub>3</sub> observations investigated in this work. Radiative transfer is calculated with a resolution of 1 nm for both the solar flux and the molecular absorption cross-sections, except between 121.4 and 121.7 nm (Lyman- $\alpha$  line) where a resolution of 0.01 nm is used (Chabrillat and Kockarts, 1997; 1998). The concentrations of long-lived species (H<sub>2</sub>, CO, N<sub>2</sub>O) are fixed at their value at 20 km but calculated by the model above 20 km. The ozone abundance at 20 km is fixed to a monthly averaged value obtained from HALOE observations (all retrievals are from version 18). This constraint is necessary as dynamics are not included. Up to about 30 km, model results for ozone are sensitive to this boundary condition and thus comparison with observations are only meaningful above 30 km. For H<sub>2</sub>O, CH<sub>4</sub>, and HCl, the profiles are derived from a monthly average of HALOE data (Harries *et al.*, 1996; Park *et al.*, 1996; Russel *et al.*, 1996) in the vicinity of Bordeaux ( $\pm 5^\circ$  in latitude and longitude) and for altitudes between 20 and 80 km. Concentrations above 80 km are calculated by the model, avoiding any extrapolation of the 80-km value for higher altitudes. Even if observations do not reach these altitudes, it is important to estimate the abundances of all absorbers influencing the radiative transfer. Monthly pressure ( $p$ ) and temperature ( $T$ ) profiles are taken from HALOE observations in the same time interval. CIRA86  $p$ ,  $T$ -profiles were used for altitudes higher than 80 km.

A first run of the model during one ‘test-year’ with mean irradiation conditions was made in order to reach a steady state for the long-lived species. Then, the model was launched with time-dependent conditions, the time step being controlled by concentration variations from  $10^{-6}$  s at sunrise and sunset up to 10 min around noon or during night. As the long-lived species are affected by non-vertical dynamics, some discrepancies are expected with real profiles. The main impact of such disagreements on ozone concentration is probably due to N<sub>2</sub>O (the main source of NO<sub>y</sub> and thus NO<sub>x</sub>) and may explain differences found with HALOE observations of NO and NO<sub>2</sub>.

Model results for comparison with O<sub>3</sub> measurements were used for the time interval from January 1995 to December 1997 in which profiles have temporal and vertical resolutions of 2 h and 5 km, respectively.

#### 3.4. THE 3-D MODEL

The chemical transport model (3-D) SLIMCAT includes the chemistry of the stratosphere, transport given by meteorological data provided by the UK Meteorological Office and a radiative transfer model. Here, the model uses a horizontal resolution of  $3.75^\circ \times 3.75^\circ$  and 12 isentropic levels between 335 and 2700 K ( $\sim 10$ –55 km).

The model output is sampled at 1200 UT for the location of the Plateau de Bure station (45°N, 10°E) in the French Alps, approximately 1000 km eastwards from Bordeaux.

## 4. Diurnal Ozone Variations

### 4.1. INTRODUCTION

Diurnal ozone variations are particularly important in the mesosphere, i.e. above approximately 50 km. At such altitudes the daily ozone cycle is governed by photodissociation processes within the odd oxygen families (e.g. Brasseur and Solomon, 1984; Allen *et al.*, 1984; Ricaud *et al.*, 1994). After sunset the ozone concentration increases rapidly due to recombination of atomic oxygen, forming ozone (Chapman, 1930). The total amount of ozone strongly depends on the existing reserve of oxygen in each altitude layer, therefore, the relative increase of ozone during the night varies with altitude. In the middle and lower stratosphere the abundance of atomic oxygen is smaller than that of ozone. In addition, the ozone lifetime exceeds one day. Thus, no or only small diurnal variations of ozone, mainly governed by the NO<sub>x</sub> family, are observed (altitude levels not shown here). For a more detailed review of the basic photochemistry in the Earth's middle atmosphere, see e.g. Allen *et al.* (1984) or Zommerfelds *et al.* (1989).

Figures 1–4 show diurnal ozone variations as an average of the years 1995–1997 for four representative months (February, May, August and November) and six altitude levels (47.5 km to 72.5 km in steps of 5 km), as measured with the Bordeaux radiometer and calculated by the 0-D and 1-D model. The model profiles are interpolated on the Bordeaux altitude grid and convolved with the Bordeaux averaging kernels in order to account for the vertical resolution (see Schneider *et al.* (2003) for details of this procedure).

### 4.2. OBSERVATIONS

Already at 47.5 km (indicating the middle altitude of the layer between 45 and 50 km) an ozone increase of typically 15% after sunset is seen in all months (Figures 1–4), relative to the mean day time value. At higher altitudes, the abundance of atomic oxygen is equal or larger than the ozone one so that the recombination reactions enrich ozone after sunset more significantly: we observe a relative increase of the daytime to night-time value of typically 30% for the 52.5-km layer, 40–60% for the 57.5-km layer, 65–120% for the 62.5-km layer, 75–200% for the 67.5-km layer, and 175–430% for the 72.5-km layer. The large range of values for the relative diurnal ozone variation for the three uppermost layers is due to a seasonal effect: the maximum amplitude for the day-night increase is found during the winter months (November, December) whereas a less pronounced variation is observed for summer (July, August). In addition, this effect is increasing with altitude as it can be seen best in Figure 4: the relative increase has its highest value (430%) for the 72.5

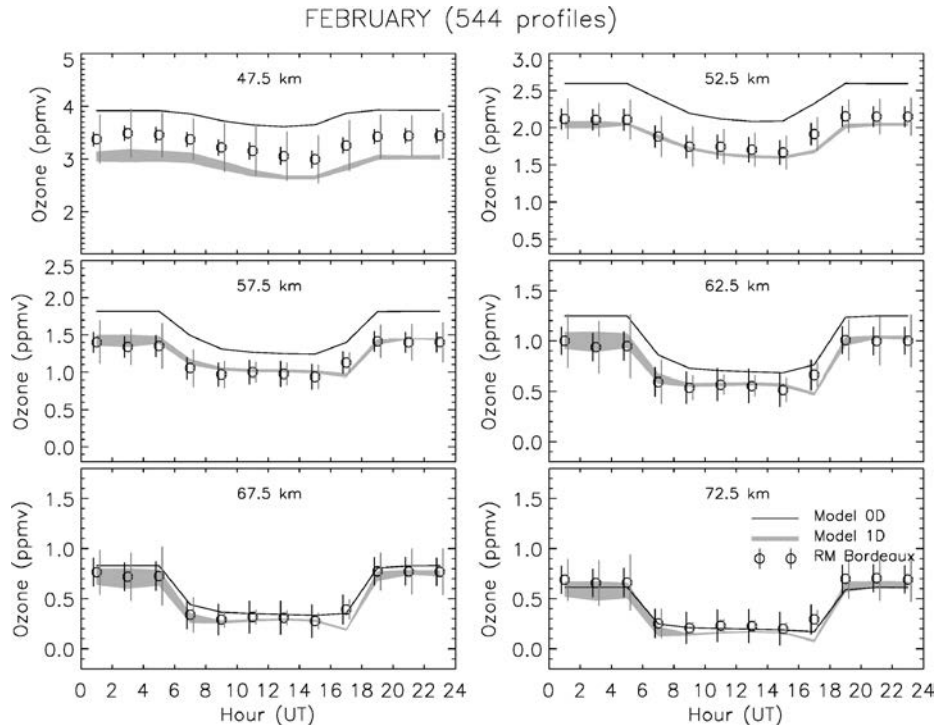


Figure 1. Diurnal variations of ozone at 6 different altitude levels for February, averaged over the years 1995–1997. The observations with the Bordeaux radiometer are indicated as circles with the black (left) bar giving the estimated error and the grey (right) bar the variability of the measurements. The results of the 0-D model are given as a solid black line, the grey shaded area represents the output of the 1-D model.

km layer. On the other hand, the 0-D and 1-D models predict less ozone for this layer in November so that one may suppose that this strong increase might be due to a problem in the observational data. But it was shown that the Bordeaux data are well validated (Schneider *et al.*, 2003) and no seasonal-dependent mismatch between Bordeaux and the data sets used for the comparison at this altitude (HALOE and the Bern radiometer for the mesosphere) was found.

#### 4.3. COMPARISON WITH MODELS

The photochemical 1-D model reproduces very well the ozone variations and the total ozone amount, except for the 62.5–72.5 km layers in November and the 47.5 km layer in February and August. The generally less satisfying modeling at 47.5 km is most likely due to the fact that at this altitude, the ozone distribution starts being dependent on dynamics, which is not included in the model. Only vertical transport of species due to molecular and turbulent diffusion is considered. However, the model contains the gas phase chemistry for 35 chemical species. The solar spectrum (taken from SUSIM observations) is used for the calculation of photodissociation rates.

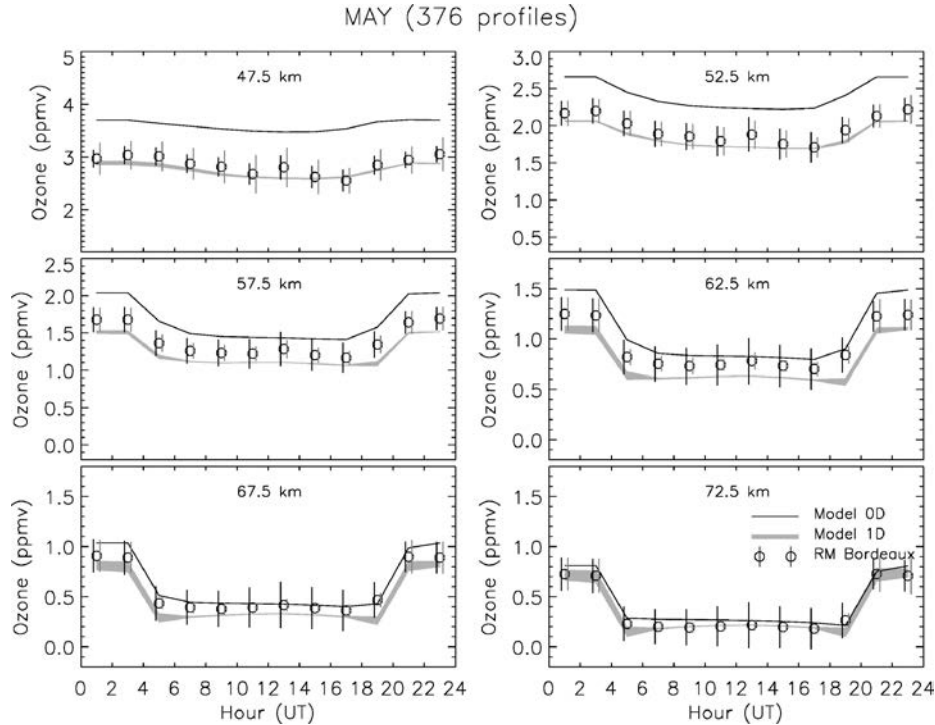


Figure 2. Same as Figure 1 but for May.

Profiles of  $\text{H}_2\text{O}$ ,  $\text{CH}_4$ , and  $\text{HCl}$  are derived from a monthly average of HALOE data (see Section 3.3 for details).

In general, the transition between dynamically and photochemically controlled region lies around 40 km. In the mesosphere the chemistry of  $\text{O}_3$  is governed by  $\text{HO}_x$  radical arising from  $\text{H}_2\text{O}$  photolysis in the upper atmosphere. In the lower mesosphere and upper stratosphere  $\text{ClO}_x$  and  $\text{NO}_x$  play a significant role. Available reaction rates and photolysis cross-sections for  $\text{NO}_x$  and  $\text{ClO}_x$  are more affected by uncertainties than for  $\text{HO}_x$  species. Thus, we note some discrepancies between the calculated  $\text{NO}$  and  $\text{NO}_2$  profiles and HALOE observations.  $\text{NO}_y$  is initialized through the model calculation of the  $\text{N}_2\text{O}$  profile and may thus also exhibit some discrepancies. The initial chlorine reservoir in our model is  $\text{HCl}$  which is constrained by observations. Quantitative diurnal variations of Cl-bearing compounds are in a reasonable agreement with observations. Thus, for altitudes at and below 45 km, we therefore expect these uncertainties to affect the modeling, even if this specific effect cannot be investigated without including 3-D transport.

We also observe a slight tendency that the ozone amount is better reproduced by the 1-D model during the day than during the *night* (e.g. the layer at 62.5 km in November, Figure 4) and that the errors for daytime modeling are smaller. The

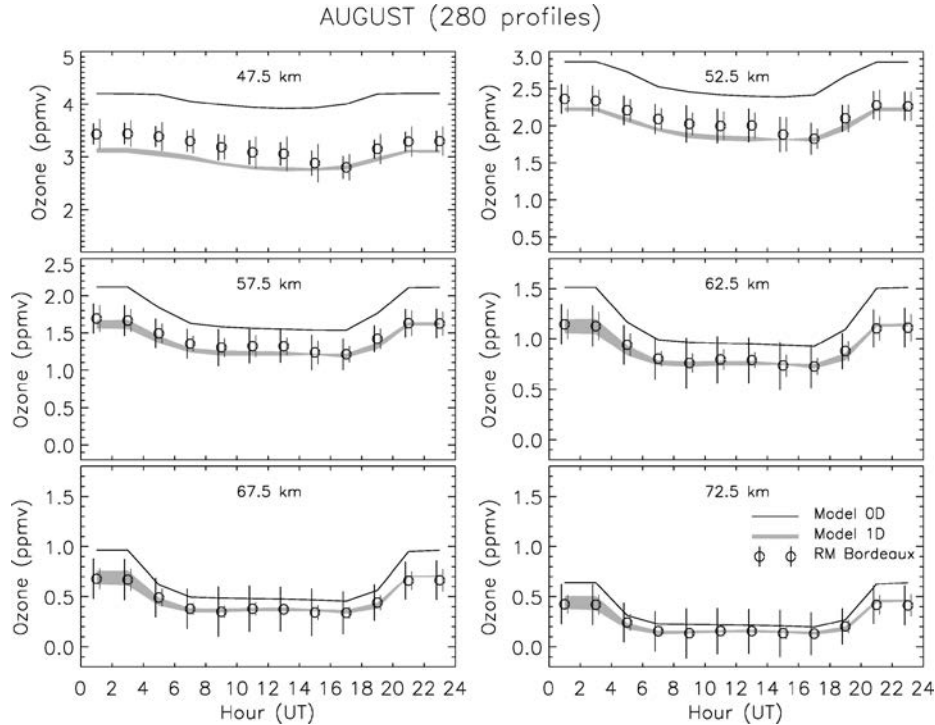


Figure 3. Same as Figure 1 but for August.

reason is that during the day photochemistry governs the reaction rates and temperature is less important which is the reverse during the night.

The good agreement between observations and the 1-D model for altitudes higher than 50 km was most likely reached by improving the following input parameters:

- (i) Water vapour profiles are taken from HALOE and are calculated above 80 km;
- (ii) a 1-nm resolution for both the solar flux and molecular cross sections (only limited by the resolution of available solar irradiance data) was used;
- (iii) a specific high resolution treatment of the Lyman- $\alpha$  line (121.5 nm), allowing an accurate calculation of H<sub>2</sub>O photolysis above 60 km;
- (iv) the temperature dependence for molecular cross sections and their quantum yield are considered in the calculations and
- (v) coupling of the altitude layers by turbulent vertical mixing which is particularly important for night-time when the chemistry is much slower.

The 0-D model generally predicts a higher ozone amount for the altitude layers 47.5–62.5 km but matches well the observations for the 67.5 km and 72.5-km layer. Exceptions are the 72.5-km layer in November where a smaller ozone vmr was predicted and the 67.5-km layer in August where a higher ozone vmr was modeled. The relative diurnal ozone variations are generally well reproduced. A comparison between the 0-D and 1-D model and observations clearly shows that

including observational data for solar flux and atmospheric species significantly improves the predictions. In particular the daily H<sub>2</sub>O profiles from HALOE are important since the atmosphere is very dry in the 0-D model (fixed H<sub>2</sub>O content) which explains the apparent O<sub>3</sub> increase.

#### 4.4. COMPARISON WITH OTHER OBSERVATIONS

The best comparison of ozone diurnal variations observed with the Bordeaux radiometer in the lower mesosphere (55 km) is provided by the mm-wave radiometer in Bern (Zommerfelds *et al.*, 1989) due to its similar vertical resolution (around 15 km) and relative proximity (both instruments are located in central Europe around 44°N). From Figures 4–6 in Zommerfelds *et al.* (1989), we obtain a relative night to daytime decrease of around 30, 70 and 80% at 55, 65, and 74 km, respectively (average over the months of December, January and April). The corresponding Bordeaux values are very similar with 35, 70, and 75% at 57.5, 67.5 and 72 km, respectively. The uncertainty of all values is around 5%. The Table Mountain Facility (TMF, Connor *et al.* (1994)) value for 55 km is equally around 30% even though one would expect a slightly smaller amplitude since TMF is located at 34°N and seasonal ozone variations strongly depend on latitude. For the northern hemisphere, Brasseur and Solomon (1984) point out that seasonal variations of *total*

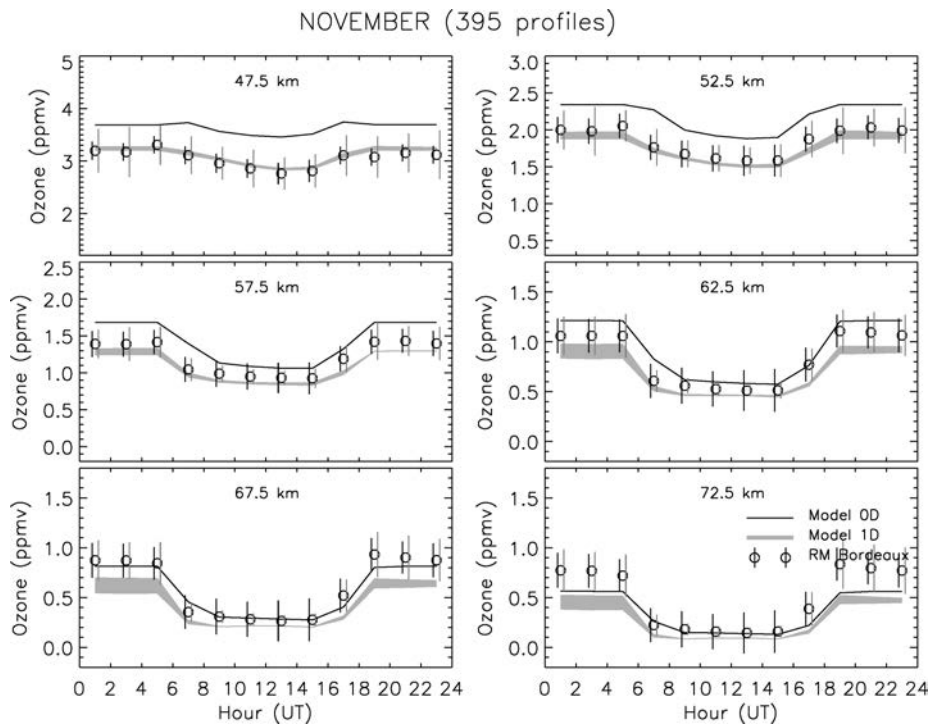


Figure 4. Same as Figure 1 but for November.

ozone become important only for latitudes higher than 30°N. At 80°N, the relative variation in total ozone is about 50%. Thomas (1990) confirm that the amplitude of ozone variations in the mesosphere (50–90 km) is increasing with latitude, having its maximum toward polar latitudes at 0.03 hPa (~72 km).

## 5. Seasonal Ozone Variations: Comparison with Models

For the analysis of the seasonal ozone variations, we use data obtained between 1995 and 1997 by the Bordeaux radiometer and HALOE. These measurements are compared to photochemical models (0-D and 1-D) and a chemical transport model (3-D), all described in Sec. 3. Due to diurnal variations of ozone in the mesosphere, day- and night-time profiles are discussed separately. We consider HALOE profiles as being taken during daytime although they are observed at sunrise and sunset (see Schneider *et al.* (2003) for a discussion of this simplification). *In contrast to Marsh et al. (2003), we do not find a differing behavior of sunrise and sunset ozone observations.* The HALOE profiles were first interpolated on the altitude grid of the Bordeaux data and then convolved with Bordeaux averaging kernels in order to assure a similar altitude resolution. Finally, all profiles were interpolated on the same pressure grid using the respective pressure and temperature profiles for each data set (monthly averages between 1995 and 1997). However, the approximate respective altitude is given for clarification. Yearly averaging cancels out interannual effects, caused by the quasibiennial oscillation (QBO) – which is marginal at mid-latitudes anyway – and ozone trends, but gives a better statistics on the seasonal cycle behaviour.

Figures 5 and 6 illustrate the observed (Bordeaux and HALOE) absolute (in ppmv) and relative (taking the yearly average as a standard) ozone variations for *day-time* observations and the model calculations. The 3-D model as a transport model is not used for the two highest altitudes. Figures 7 and 8 show in the same way the Bordeaux *night-time* observations (no HALOE measurements) and the model calculations for the 0-D and 1-D models. The error of the Bordeaux data is the weighted mean of variable and systematic errors (Schneider *et al.*, 2003) and is indicated as an errorbar in Figure 5 (the values for night-time observations are the same).

We distinguish the altitude ranges: middle and upper stratosphere, and mesosphere which will be discussed in the following sections.

### 5.1. MIDDLE STRATOSPHERE (26–40 KM OR 23–3 HPA)

At the pressure levels 23 and 6 hPa (corresponding to ~26 and ~35 km) observations indicate a pronounced annual oscillation (AO) with a minimum during the autumn-winter period and a maximum in spring-summer both for day- and night-time profiles. The amplitude of the AO at 26 km is of the order of 15% (all variations given in this paper in percentages are total values), see Figure 6 and 8, which is in agreement with lidar observations at OHP/France (Guirlet *et al.*, 1997) and ozone sonde observations at Hohenpeissenberg/Germany (Hassler *et al.*, 2003).

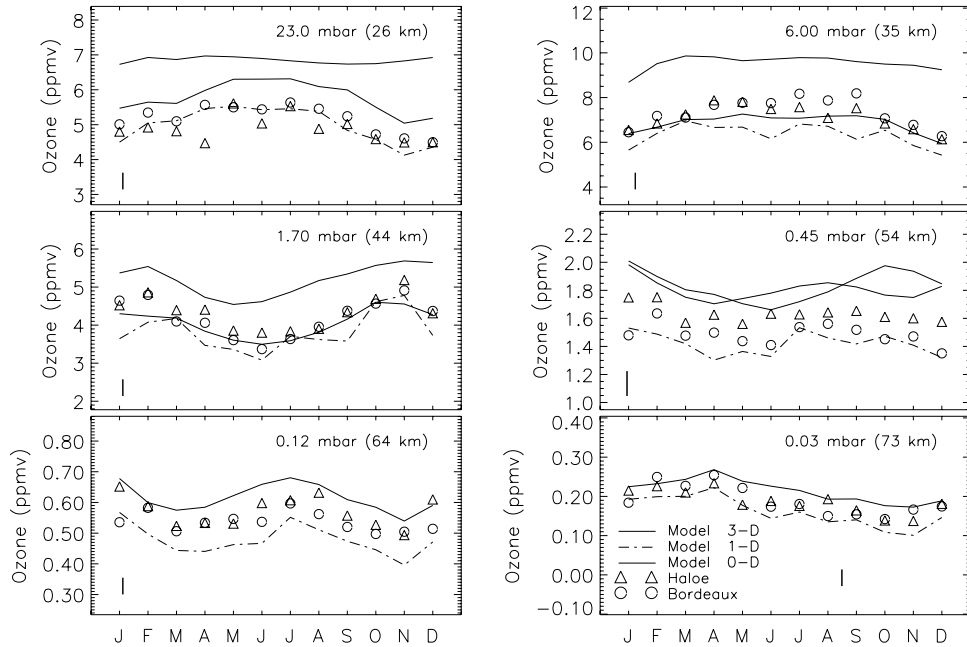


Figure 5. Absolute seasonal variations for the daytime ozone profiles at 6 different pressure levels observed by the Bordeaux ozone radiometer (circles) and HALOE (triangles) and as calculated by two photochemical models (0-D, solid line and 1-D, dashed-dotted line) and a chemical transport model (3-D, dash-dot-dot-dot line). The approximate altitude is given for clarification. The typical error of the Bordeaux data for one month is indicated as a vertical line in the lower corner of the plot. It is the weighted mean over one month averaging the years 1995–1997 and including variable and systematic errors. The error varies only slightly between each month so that we give only the mean instead of errorbars for each month.

In this altitude range and at this latitude, the summerly ozone maximum is mainly due to mean meridional transport of ozone-rich air from the tropics (Cordero and Kawa, 2001; Tsou *et al.*, 1995). On the other hand, around 35-km ozone variations start to be photochemically controlled and the observed seasonal cycle can partly be explained by the annual change in solar flux. At mid-latitudes, ozone production and destruction are approximately balanced by transport, while at higher latitudes ( $40^\circ$  polewards) and between 15 km and 30 km, a net ozone loss during summer is due to photochemical destruction (Cordero and Kawa, 2001).

The transport model (which includes photochemistry as well) reproduces correctly the relative daytime variability at 26 km and 35 km as seen in Figure 6. The absolute ozone amount at 26 km (Figure 5), however, is only marginally well reproduced. The 0-D model, where the  $H_2O$  contents do not vary seasonally, shows a nearly constant ozone field over 12 months at 26 km and 35 km

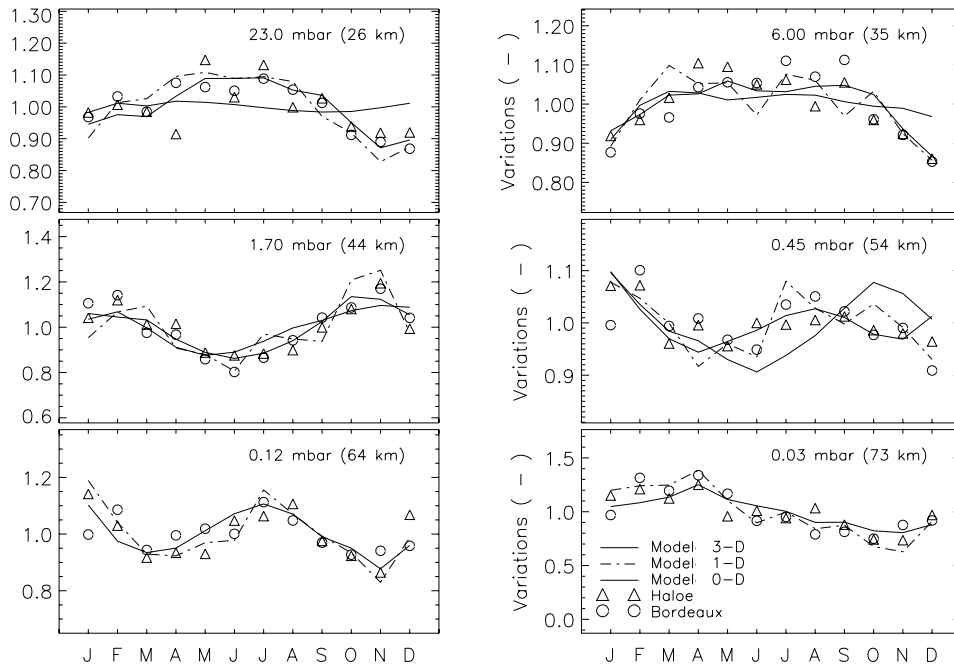


Figure 6. Same as Figure 5 but for variations relative to the 1995–1997 average daytime ozone profiles.

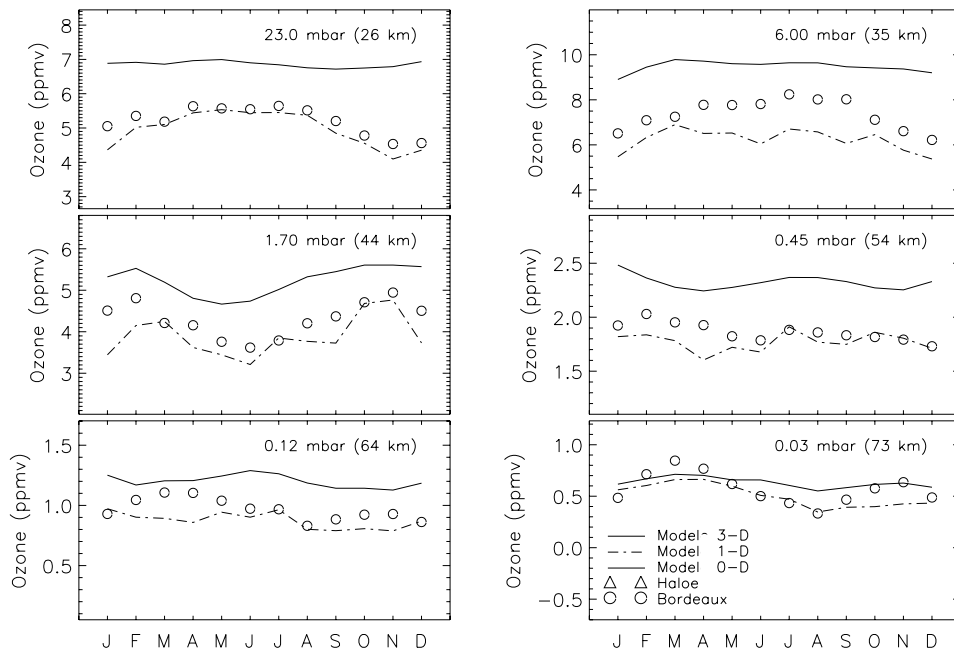


Figure 7. Same as Figure 5 but for night-time ozone profiles.

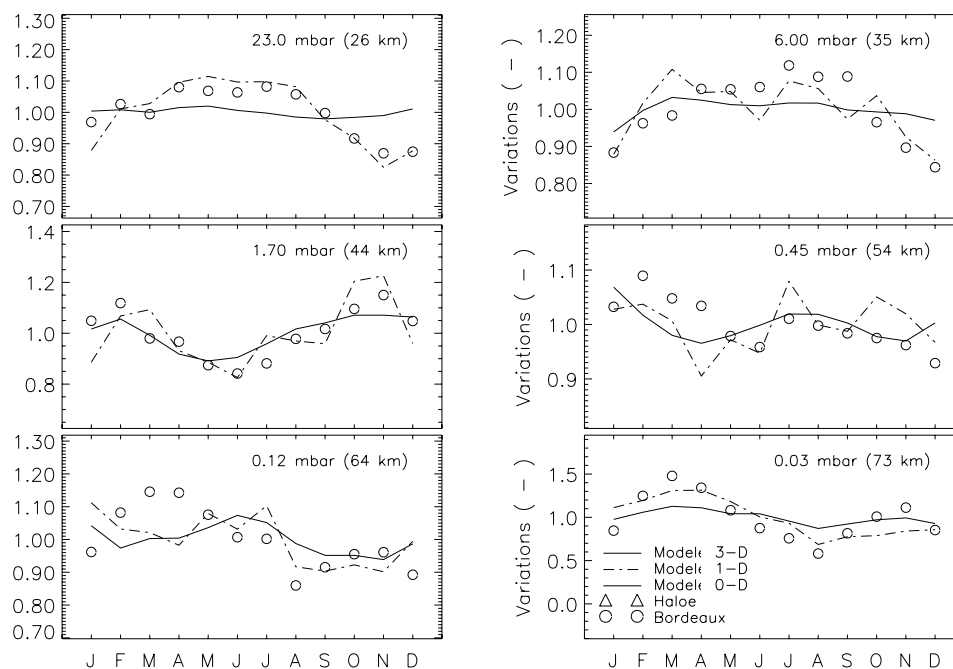


Figure 8. Same as Figure 7 but showing the relative variations for night-time ozone profiles.

but starts to model correctly the ozone variability at 44 km. The absolute ozone amounts are, however, overpredicted. The 1-D model results for the 26-km level are mainly governed by HALOE ozone observations and should be treated with care. At 35 km, the influence of HALOE observations is much smaller. While the relative variations are very well reproduced, the absolute ozone amount is slightly underestimated.

To which extent the ozone variability in the lower/middle stratosphere is also caused by effects like the 2-year QBO, the 11-year solar cycle and the El Nino-Southern Oscillation (ENSO) cannot be judged from our observations (see Hassler *et al.* (2003) for a quantitative discussion of these effects for observations at Hohenpeissenberg). Appenzeller *et al.* (2000) showed that a part of the multiannual variability in total ozone (which is mainly constituted by the vertical ozone column below 35 km, (Brasseur and Solomon, 1984)) in Northern middle and high latitudes is linked to changes in the dynamical structure of the atmosphere related to the North Atlantic Oscillation (NAO). A similar influence of the Arctic Oscillation was found by Thompson *et al.* (2000). See Jaehelin *et al.* (1992) for a more detailed discussion.

Nearly no differences for the amplitude of the annual ozone cycle in the altitude range 30–40 km is indicated by lidar observations at Hohenpeissenberg (Hassler *et al.*, 2003): the relative variation is 17, 18, 18 % at 30, 35, and 40 km, respectively, in very good agreement with the Bordeaux values.

## 5.2. UPPER STRATOSPHERE (40–50 KM OR 3–1 HPA)

At the 1.7 hPa ( $\sim 44$  km) level, we see a strong tendency for a semi-annual oscillation with a pronounced ozone minimum in summer and a weaker one in winter (December/January). The absolute amplitude of the variation of  $\sim 20\%$  is significant and was also observed by e.g. McDermid *et al.* (1990) with a lidar and SAGE-II (18% and 27% variation at 40 km and 45 km, respectively). The main reason for the ozone summer minimum at this altitude is probably the increase of the reaction rates of odd-hydrogen and odd-oxygen – which destroy ozone – due to higher stratospheric temperatures during summer (Perliski *et al.*, 1989, Brasseur and Solomon, 1984, Tsou *et al.*, 1995). However, an ozone decrease due to an opposite water vapour cycle can not be ruled out as we will show in Section 5.4. In this case, water photolysis produces hydrogen species which are responsible for the destruction of ozone (Brasseur and Solomon, 1984). Meridional circulation then transports this air containing more water vapour to higher altitudes so that – as was shown by models – the response of ozone to water vapour variability is largest in the upper mesosphere between 75 km and 80 km (Marsh *et al.*, 2003).

All models reproduce well the relative variations (Figures 6–8), though only the 1-D model shows a significant winter minimum. The 0-D model over-estimates the total ozone abundance whereas the 1-D and 3-D models reproduce well summer values but underestimate the ozone amounts between December and February. A general problem for the photochemical models (*0-D and 1-D*) at this altitude and above is that the ozone content is partly under indirect dynamic influence: even if the ozone abundance is primarily controlled photochemically, some long-lived species like, e.g.,  $\text{H}_2\text{O}$ , which odd derivatives lead to a destruction of ozone, are dynamically driven. Therefore, pure photochemical models reach their limit in modeling correctly all details of diurnal and seasonal ozone variations. On the other hand, even photochemical-radiative-dynamical models (Brasseur *et al.*, 1990; Huang, 1994; Chen, 1994) are not able to model realistically ozone *trends* (DeToma *et al.*, 1996) in the upper stratosphere and lower mesosphere. Thus, it is not only the missing dynamical compounds in the photochemical models which account for the discrepancies found.

## 5.3. LOWER MESOSPHERE (50–65 KM OR 1–0.1 HPA)

The lower mesosphere is characterized by the 0.45 and 0.12 hPa levels ( $\sim 54$  and  $\sim 64$  km). The Bordeaux and HALOE data at 54 km do not give a very clear picture. A tendency for a SAO is found with ozone minima (maxima) in December/January and May/June (February and July) with the February maximum being larger than the July one. The amplitude of the oscillations is typically 10–15% at 54 km (and therefore just above the error level of the data) but increases to 10–20% for 64 km (Figures 6 and 8). The same variation was observed by the Solar Mesosphere Explorer (SME) in the altitude range 50–90 km (Thomas *et al.*, 1984; Thomas, 1990).

Daytime observations at 64 km (Figures 5 and 6) show very pronounced ozone minima (maxima) in spring and autumn (summer and winter) but the night-time observations reveal an unexpected reversal of this cycle (Figures 7 and 8) with a maximum in spring. There is no physical reason why day- and night-time seasonal cycles should be different (as also seen in the model predictions) so that we attribute this discrepancy to a problem in the Bordeaux data. From Figure 10d in Schneider *et al.* (2003), it gets obvious that night-time Bordeaux ozone data at this altitude are 30% lower than comparable data from the Bern radiometer, pointing towards a possible calibration problem for night-time observations. A very clear semi-annual cycle for night-time observations was detected in data of a mm-wave radiometer located in Tsukuba, Japan ( $36.1^\circ$ , Nagahama *et al.*, 2003). At an altitude of 60 km, a SAO with an amplitude of  $\pm 13\%$  was found.

The semi-annual ozone oscillation was initially explained (Garcia and Solomon, 1985) by an opposite phase variation of water vapour, which would be consistent with a mainly diffusive atmosphere (Bevilacqua *et al.*, 1990). Observations by Olivero (1986), Tsou *et al.* (1988), and Nedoluha *et al.* (1998) however, show so far no clear semi-annual water vapour variation in the mesosphere. A significant semi-annual water vapor cycle at high altitudes ( $> 70$  km) was reported by Nedoluha *et al.* (1996) from observations at  $45^\circ$ S (Lauder/New Zealand) while at  $34^\circ$ N (Table Mountain/USA) is it much weaker. They also observed an increase of the amplitude of the cycle with altitude.

Our analysis of HALOE water vapour data at altitudes between 40 km and 60 km, however, show indeed a disposition of an opposite water cycle (see Section 5.4 for a discussion) which may contribute to the observed ozone variability. Other studies (Siskind *et al.*, 2002), also using HALOE data but in a different latitude range and time interval, did not reveal this anticorrelation between  $O_3$  and  $H_2O$ . Bevilacqua *et al.* (1990) suggest local photochemistry and/or variations in the horizontal transport of atomic oxygen to explain the observed ozone SAO. That holds, however, mainly for the upper mesosphere region. Nagahama *et al.* (2003) suggest that seasonal variations of temperature and solar flux may cause the semi-annual ozone variation.

The 1-D model reproduces acceptably well the relative ozone variation at 54 km and 64 km for daytime. Due to a possible problem in the Bordeaux night-time data at 64 km, we do not discuss this altitude. The weak winter minimum at 54 km in January and December is reproduced by the 3-D and 1-D models. Small discrepancies between observations and 1-D model results can be due to the fact that the observational  $H_2O$  profiles from HALOE were monthly averaged and that there are uncertainties in the photochemical data, mainly with respect to the temperature dependence of the photolysis cross sections of  $O_3$  and  $H_2O$ . Interestingly, the 0-D model with its constant water vapour profile fails to reproduce the 54 km ozone variability. This implies that yearly changes in water vapour at this altitude may indeed have an influence on the ozone content. The 3-D model generally overestimates the total ozone abundance and shows a seasonal peak in October/November which

is not visible in the observations. At this altitude, however, the model assumes the  $O_x$ -,  $HO_x$ - and  $ClO_x$ - families to be in photochemical equilibrium which is not the case.

Summarizing the results obtained so far, we conclude that a strong SAO is seen at 44 km, no clear SAO at 54 km and again a SAO – but with reversed phase compared to the one at 44 km – at 64 km. However, it is problematic to interpret such data due to the low altitude resolution of the observations which is around 15 km. Ozone vmrs of different atmospheric layers are mixed so that a phase reversal of the SAO between 44 and 64 km causes the ozone vmr at the altitude layers in between to be more scattered. In order to address this problem, we use here high resolution (2 km) HALOE data to investigate in more detail the altitude range 44–64 km.

#### 5.4. HIGHER RESOLUTION ANALYSIS OF HALOE OZONE AND WATER VAPOUR DATA BETWEEN 44 AND 64 KM

##### 5.4.1. Ozone Data

The Halogen Occultation Experiment (Russel *et al.*, 1996) provides high vertical resolution (1–2 km) ozone profiles in the altitude range 10–90 km. Here, we selected data with tangent point coordinates within a rectangle of  $15^\circ$  in latitude and  $7^\circ$  in longitude centering Bordeaux and observed between 1995 and 1997 to produce monthly averaged profiles (see Schneider *et al.* (2003) for a validation analysis of HALOE data using the Bordeaux radiometer).

Figure 9 displays relative (with regard to the yearly average) ozone variations at nine altitude layers between 43 and 64 km, approximately separated by steps of 2 km. Between 43 and 48 km, a SAO with a minimum in summer (May–August) and December/January is clearly visible. A November maximum is equally prominent but the spring maximum breaks up in a double-peak feature (February and April). The following altitude layer at 51 km shows no clearly defined minima and maxima at different seasons but monthly fluctuations. The next three altitude levels (54, 56 and 59 km) all show an ozone minimum in October/November with a sharp increase of ozone until February. Interestingly there is no defined spring or summer minimum, moreover, ozone values gradually decrease until November. At higher altitudes (62 km and 64 km), the November minimum is even stronger with a sharp re-increase of ozone in December and another minimum in February. The peak month of the summer maximum depends on the altitude: it is in July/August for the 62 km level and May for the 64 km level.

Thus, we can conclude that there is indeed a clearly visible phase reversal of the SAO between 44 and 64 km which was smeared out in the lower resolution Bordeaux observations. Upcoming high-quality data from the Odin satellite (Murtagh *et al.*, 2002) with typically 2 km altitude resolution thus allow an even more detailed analysis of the ozone variations in this altitude range.

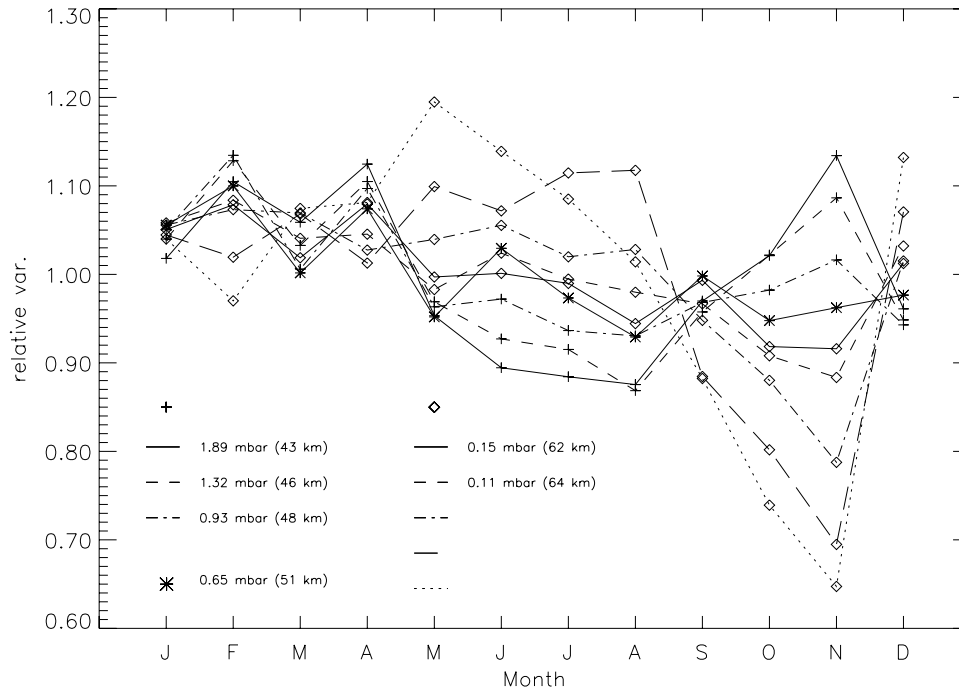


Figure 9. Relative ozone variations for monthly averaged (1995–1997) daytime ozone profiles obtained with HALOE. The crosses and the diamonds define two different regimes of the SAO: the crosses (subdivided in to the altitude levels 43, 46, and 48 km by different line types) mark the summer minimum and November maximum cycle whereas the diamonds (also separated by different line types in  $\sim 2$  km steps between 54 and 64 km altitude) define the typical November minimum cycle. The asterisks indicates the 51 km level which is not assigned to one of the two regimes.

#### 5.4.2. Water Vapour Data

In order to explore the possibility that the seasonal ozone variability seen in the altitude range  $\sim 40$  to  $\sim 65$  km is due to an opposite phase shift of water vapour, we plot HALOE water vapour and ozone measurements together in Figure 10. We use the same ozone data already shown in Figure 9 but additionally vertically averaged over the altitude ranges identified there. The same was done for water vapour measurements, HALOE sunrise and sunset data from 1995–1997 were monthly and vertically averaged and finally normalized. We exclude the range 48–54 km since no clear ozone variability was seen.

For the altitude intervals 43–48 km and 54–59 km, a weak anticorrelation for water vapour and ozone is seen, the altitude range 60–65 km shows a tendency for a correlation (except of the summer months). All values have to be treated with care since the absolute variations are small. They are of the order of 10%, except the strong ozone November minimum at 60–65 km and the water vapour semi-annual variability (maxima in summer and winter) at the same altitude range. As a result,

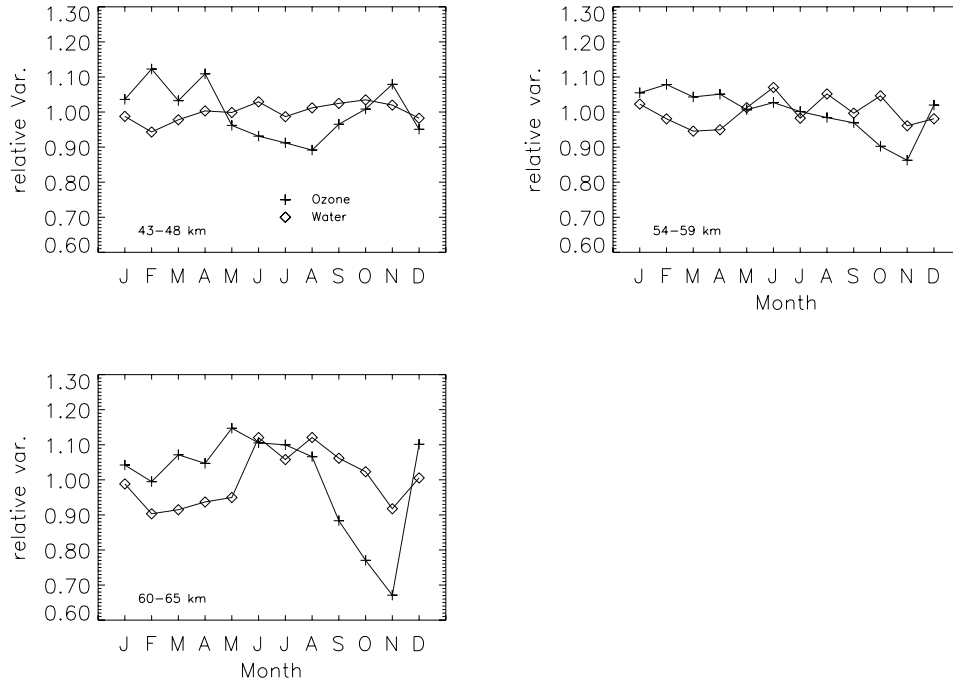


Figure 10. Relative ozone and water vapour variations for monthly averaged (1995–1997) ozone (crosses) and H<sub>2</sub>O (diamonds) profiles obtained with HALOE. Data are shown as altitude averages over the 3 regimes defined in Fig. 9: 43–48 km, 54–59 km, and 60–65 km.

we are reluctant to explain the observed SAO in the upper stratosphere and lower mesosphere (up to 60 km) only due to water vapour changes.

### 5.5. UPPER MESOSPHERE (65–75 KM OR 0.1–0.02 hPa)

The 0.03-hPa level ( $\sim 73$  km) represents the upper mesosphere. A SAO with minima at solstices and maxima at equinoxes is recognized clearly in night-time observations but is less evident in daytime data. The observed amplitudes are large, reaching up to 50% in total while the SAO observed with the Japanese mm-wave radiometer (Nagahama *et al.*, 2003) has a maximum value of  $\pm 28\%$ . Since a high photolysis rate makes ozone very short lived at this altitude, the ozone abundance is most likely to a large part due to the photochemical coupling between ozone and temperature. Clancy and Rusch (1989), e.g., derived annual temperature variations with a peak in January and a minimum in June. Accordingly, the photochemical models explain well not only the amplitude of the variations but also the absolute amount of ozone. Water vapour variations, as they were suggested by Marsh *et al.* (2003) as an explanation of the ozone SAO do not necessarily hold since the ozone cycle and amount are well reproduced by the 0-D model which is using a constant water vapour profile for the whole year. Decisive factors are probably solar flux and in

particular temperature which was already recognized by Allen *et al.* (1984) and Nagahama *et al.* (2003). Since solar radiation, temperature and pressure as input are different for the 0-D and 1-D models, slight differences in the prediction of absolute ozone values are explained.

## 6. Summary

Ozone volume mixing ratios, observed with the Bordeaux microwave radiometer between 1995 and 1997, show diurnal variations in the mesosphere and seasonal variations in the stratosphere and mesosphere.

The daily ozone variability was investigated by taking the average of the years 1995–1997 for four months and six altitude levels (47.5–72.5 km by steps of 5 km). We observe a relative increase of the daytime to night-time value between 20% for the 47.5 km layer and 175–430% for the 72.5 km layer. The maximum amplitude is found during the winter months and at the highest altitudes. Comparing the amplitude at 52.5 km with observations obtained with other radiometers showed a very good agreement within 1%.

Observations were compared to two photochemical models: a 0-D model with a constant H<sub>2</sub>O profile over the whole year, and a 1-D model, considering vertical transport by molecular and turbulent diffusion and using observational data of the solar flux, temperature, pressure and H<sub>2</sub>O. Generally, the photochemical 1-D model reproduces well ozone variations and the total ozone amount at all altitude levels except the lowermost one where the ozone distribution starts to be governed by dynamics. We think that the more accurate predictions of the 1-D model are mainly due to an improved treatment of water vapour profiles and solar flux, i.e. taking observational data as input, and the more precise radiative transfer at high spectral resolution using temperature-dependent photodissociation cross sections.

Seasonal ozone variations were seen by the Bordeaux radiometer as an annual oscillation (AO) in the middle stratosphere (26–40 km) and a semi-annual oscillation (SAO) in the upper stratosphere (40–50 km) and mesosphere (50–75 km). Due to the ozone diurnal variation, we distinguish between day- and night-time profiles.

At ~26 km and ~35 km, an AO with a minimum during the autumn-winter period and a maximum in spring-summer is observed. The amplitude of the AO at 26 (35) km is of the order of 10% (15%), which is confirmed by other observations. Mainly transport phenomena are responsible for this cycle whose relative variations are correctly modeled using a 3-D transport model (SLIMCAT). However, at 35 km, ozone variations also start to be photochemically controlled and the observed seasonal cycle can partly be explained by the annual change in solar flux. Accordingly, the 0-D and 1-D models explain correctly the relative ozone variations at this altitude. A SAO is observed at the 1.7 hPa (~44 km) level with a summerly ozone minimum originating presumably from an increase of reaction rates of odd-hydrogen and odd-oxygen due to higher stratospheric temperatures in summer.

The mesospheric ( $\sim 54$ ,  $\sim 64$  km) ozone variability is characterized by a semi-annual oscillation. Daytime measurements show ozone minima (maxima) approximately in December/January and May/June (February and July). A phase reversal in the SAO between the 44 and 64 km levels was clearly seen in high resolution (2 km) HALOE observations. There is yet no generally accepted theory for the SAO in the mesosphere. Phase variations of water vapour are discussed, as well as local photochemistry and/or variations in the horizontal transport of atomic oxygen. A simple explanation for the SAO would be seasonal variations of temperature and solar flux. Both, the 0-D and 1-D models reproduce well the relative ozone variation for daytime observations which is remarkable since the 0-D model uses a constant H<sub>2</sub>O profile. But only the 1-D model reproduces correctly the observed SAO phase reversal with an ozone minimum (maximum) in November at 64 (44) km.

Summarizing, we come to the conclusion that the 1-D model is best suited to predict diurnal and seasonal variations of ozone in the Earth's atmosphere above around 30 km. It shows some significant improvements with regard to other models and offers promising perspectives to model extraterrestrial planet's atmospheres (Selsis *et al.*, 2002; Rontó *et al.*, 2003).

### Acknowledgements

This work was funded in France by the *Institut National des Sciences de l'Univers* (INSU), C.N.R.S., and the *Programme National de Chimie Atmosphérique* (PNCA). The radiometer is operated thanks to national funds of the *Ministère de l'Education Nationale/Université Bordeaux I* (Contract NDSC). European funds supported Dr. N. Schneider through contract Nr. ENV4-CT98-0750 entitled *Compilation of atmospheric Observations in support of Satellite measurements over Europe* (COSE). Mr. W. D'Anna was supported by a CNRS contract.

The authors wish to thank Dr. Martyn Chipperfield of the *School of Environment, University of Leeds*, United Kingdom for his kind contribution of model results.

### Notes

1. HALogen Occultation Experiment onboard the upper atmosphere research satellite (UARS).
2. Microwave limb sounder onboard UARS.
3. Stratospheric aerosol and gas experiment II onboard the earth radiation budget satellite.
4. We call this code a 0-D or box model since vertical transport is not included. However, transfer of dissociative radiation according to a vertical distribution of species is comprised.
5. Solar ultraviolet spectral irradiance monitor.
6. Upper atmosphere research satellite.

### References

- Allen, M., Lunine, J. I., and Yung, Y. L., 1984: The vertical distribution of ozone in the mesosphere and lower thermosphere, *JGR* **89**, 4841.

- Appenzeller, C., Weiss, A., and Staehlin, J., 2000: NAO modulated total ozone winter trends, *GRL* **27**, 1131–1134.
- Barnett, J. J. and Corney, M., 1985: Middle atmosphere reference model derived from satellite data, *Handbook for MAP* **16**, 47–85.
- Bevilacqua R. M., Strobel D. F., Summers M. E., Olivero J. J., and Allen M. 1990: The seasonal variation of water vapour and ozone in the upper mesosphere, *JGR* **95**, 883–893.
- Bjarnason, G. G., Solomon, S., and Carcia, R. R. 1987: Tidal influences on vertical diffusion and diurnal variability of ozone in the mesosphere, *JGR* **92**, 5609–5620.
- Brasseur, G. and Simon, P. 1981: Stratospheric chemical and thermal response to long-term variability in solar UV irradiance, *JGR* 7343–7352.
- Brasseur, G. and Solomon, S., 1984: *Aeronomy of the Middle Atmosphere*, D. Reidel Publishing Company.
- Brasseur, G., Hitchman, M. H., and Walters, S., et al. 1990: An interactive chemical dynamical radiative 2-D model of the middle atmosphere, *JGR* **95**, 5639–5649.
- Chabrilat, S. and Kockarts, G., 1997: Simple parameterization of the absorption of the solar Lyman- $\alpha$  line, *GRL* **24**, 2659.
- Chabrilat, S. and Kockarts, G., 1998: Simple parameterization of the absorption of the solar Lyman- $\alpha$  line, *GRL* **25**, 79.
- Chapman, S., 1930: A theory of upper atmospheric ozone, *Mem. Royal. Meteorol. Soc.* **3**, 130.
- Chen, L., 1994: Middle atmosphere ozone response to solar UV variations, *Ph.D. thesis*, University of Colorado.
- Chipperfield, M. P., Santee, M. L., and Froidevaux, L., et al., 1996: Analysis of UARS data in the southern polar vortex using chemical transport model, *JGR* **101**, 18861–1881.
- Clancy, R. T., Rusch, D. W., and Thomas, R. J., et al., 1987: Model ozone photochemistry on the basis of SME mesospheric observations, *JGR* **92**, 3067–3080.
- Clancy, R. T. and Rusch, D. W. 1989: Climatology and trends of mesospheric temperatures, *JGR* **94**, 3377–3393.
- Cordero, E. C. and Kawa, S. R. 2001: Ozone and tracer transport variations in the summer Northern Hemisphere stratosphere, *JGR* **106**, 12227–12239.
- Connor, B. J., Siskind, D. E., and Tsou, J. J., et al. 1994: Ground-based microwave observations of ozone in the upper stratosphere and mesosphere, *JGR* **99**, 16757–16770.
- de La Noë, J., Lezeaux, O., Guillemin, G., Lauqué, R., Baron, P., and Ricaud, P. 1998: A ground-based microwaveradiometer dedicated to stratospheric ozone monitoring, *JGR* **103**, 22147–22161.
- DeToma, G., London, J., and Chen, L., et al. 1996: Solar cycle changes in UV irradiance, in *Proceedings of the XVIII Quadrennial Ozone Symposium*. Vol. **1**, p. 259.
- Eluszkiewicz, L. and Allen, M. 1993: A global analysis of the ozone deficit in the upper stratosphere, *GRL* **98**, 1069.
- Floyd, L. E., Reiser, P. A., and Crane, P. C. et al. 1998: Solar cycle 22 UV spectral irradiance variability: Current measurements, *Sol. Phys* **177**, 79.
- Froidevaux, L., Allen, M., and Berman, S., et al. 1985: A critical analysis of ClO and O<sub>3</sub>, *GRL* **90**, 12999–13029.
- Garcia, R. R. and Solomon, S. 1985: The effect of breaking gravity waves, *JGR* **90**, 3850–3852.
- Guirlet, M., Keckhut, P., Godin, S., and Mégie, G., 1997: Long-term monitoring and trends of stratospheric ozone at OHP, *Air pollution research report, European Commission* **73**, p. 83.
- Hassler, B., Steibrecht, W., and Winkler, P., et al. 2003: Trends and interannual variations of stratospheric ozone and temperature in observations and chemistry-climate models, *Proceedings of EGS 2003*, CD-ROM.
- Harries, J. E., Russell, J., and Tuck, A. F., et al., 1996: Validation of measurements of water vapour from the HALogen Occultation Experiment, *JGR*. **101**, 10205–10225.

- Huang, Y. W. H. 1994: The response of the middle atmosphere to external perturbations, *Ph.D. Thesis*, University of Michigan.
- Huang, Y. W. H., Reber, C. A., and Austin, J., 1997: Ozone diurnal variations observed by UARS and their model simulation, *JGR* **102**, 12971–12985.
- Huebner, W. F., Keady, J. J., and Lyon, S. P. 1992: Solar photo rates for planetary atmospheres and atmospheric pollutants, Kluwer Academic Press.
- Jaehelin, J., Harris, N. R. P., and Appenzeller, C., et al. 2001: Ozone trends: A review, *Rev. Geophys.* **39**, 231–290.
- Marsh, D., Smith, A., and Noble, E., 2003: Mesospheric ozone response to changes in water vapour, *JGR* **108**, D3, 4109.
- McDermid, I. S., Godin, S., and Lindquist, L. O., 1990: Ground-based laser DIAL system for long term measurements of stratospheric ozone, *Appl. Optics* **29**.
- Murtagh, D., Frisk, U., and Merino, F. et al., 2002: An overview of the ODIN mission, *Can. J. Phys.* **80**, 4, 309–319.
- Nagahama, T., Nakane, H., and Fujinuma, Y. et al. 2003: A semi-annual variation of ozone in the middle mesosphere observed with the mm-wave radiometer at Tsukuba, Japan, *JGR, in revision*.
- Nedoluha, G. E., Bevilacqua, R. M., and Gomez, R. M., et al. 1996: Measurements of water vapor in the middle atmosphere and implications for mesospheric transport, *JGR* **101**, D16, 21183.
- Nedoluha, G. E., Bevilacqua, R. M., and Gomez, R. M. et al. 1998: Increases in middle atmospheric water vapor as observed by HALOE and the WVMS from 1991 to 1997, *JGR* **103**, D3, 3531–3543.
- Olivero, J. J., Tsou, J. J., and Croskey, C. L., et al. 1986: Solar absorption microwave measurements of upper atmospheric water, *GRL* **13**, 197.
- Pallister, R. C. and Truck, A. F. 1983: The diurnal variation of ozone in the upper stratosphere as a test of photochemical theory, *Q.J.R. Meteorol. Soc.* **109**, 271–284.
- Park J. H., Russell J. M. I., and Gordley L. L., et al. 1996: Validation of HALogen Occultation Experiment CH<sub>4</sub> measurements from the UARS, *JGR* **101**, 10183–10199.
- Perliski, L., Solomon, S., and London, J. 1989: On the interpretation of seasonal variations of stratospheric ozone, *Planet. Space Sci.* **37**, 12, 1527–1538.
- Rees, D., Barnett, J. J., and Labitzke, K. (eds.), 1990: COSPAR International Reference Atmosphere (CIRA) Part II: Middle Atmosphere Models, Pergamon Press, Oxford, England.
- Ricaud, P., Brillet, J., de la Noë, J., and Parisot, J. P. 1991: Diurnal and Seasonal Variations of Stratospheric Ozone, *JGR* **96**, 18617–18629.
- Ricaud, P., Brasseur, G., Brillet, J., and de la Noë, J., et al. 1994: Theoretical validation of ground-based mm ozone observations, *Ann. Geophys.* **12**, 664–673.
- Ricaud, P., de la Noë, J., and Connor, B., et al. 1996: Diurnal variability of mesospheric ozone as measured by UARS, *JGR* **101**, 10077–10089.
- Rodgers, C. D. 1976: Retrieval of atmosph. temperature and composition from remote measurements of thermal radiation, *Rev. Geophys. Space Sci.* **14**, 609–624.
- Rontó, Gy., Bérces, A., and Lammer, H., et al. 2003: Solar UV irradiation conditions on the surface of Mars, *Photochem. Photobiol.* **77-1**, 34–40.
- Russell, J. M. I., Deaver, L. E., and Luo, M., et al., 1996: Validation of hydrogen chloride measurements made by HALOE from the UARS Platform, *JGR* **101**, 10151–10161.
- Sander, S. P., Friedl, R. R., and DeMore, W. B., et al. 2000: Chemical kinetics and photochemical data for use in stratospheric modeling – Evaluation number 13, *NASA/JPL Publications*.
- Schneider, N., Lezeaux, O., de La Noë, J., Urban, J., and Ricaud, P. 2003: Validation of Ground-based Observations of Strato-Mesospheric Ozone, *JGR* **108**, D17, 4540.
- Selsis, F., 2000: Evolution model of the atmosphere of terrestrial planets, *Thèse Doctorat, Université Bordeaux I*.
- Selsis, F., Despois, D., and Parisot, J.-P., 2002: Signature of life on exoplanets: Can Darwin produce false positive detections?, *Astron. Astrophys.* **388**, 985–1003.

- Siskind, D. E., Nedoluha, G., Summers, M. E., and Russell, J. M. 2002: A search for an anticorrelation between H<sub>2</sub>O and O<sub>3</sub> in the lower mesosphere, *JGR* **107**, D20, 4435.
- Thomas, R. J., Barth, C. A., and Solomon, S. 1984: Seasonal variations of ozone in the upper mesosphere and gravity waves, *GRL* **11**, 673.
- Thomas, R. J. 1990: Seasonal ozone variations in the upper mesosphere, *JGR* **95**, 7395–7401.
- Thompson, D. W., Wallace, J. M., and Hegerl, G. C. 2000: Annular mode in extratropical circulation, part II, *J.Clim.* **13**, 1018.
- Tsou, J. J., Olivero, J. J., and Croskey, C. L. 1988: A study of the variability of H<sub>2</sub>O during spring 1984, *JGR* **93**, 5255–5266.
- Tsou, J. J., Connor, B., J., and Parrish, A., et al. 1995: Ground-based microwave monitoring of middle atmosphere ozone, *JGR* **100**, 3005–3016.
- Zommerfelds, W. C., Künzi, K. F., and Summers, M. E., et al. 1989: Diurnal variations of mesospheric ozone obtained by ground-based microwave radiometry, *JGR* **94**, 12819–12832.